

UC Irvine

UC Irvine Previously Published Works

Title

Development of chiral fluorinated alkyl derivatives of emixustat as drug candidates for the treatment of retinal degenerative diseases.

Permalink

<https://escholarship.org/uc/item/3wk111pb>

Journal

Bioorganic and Medicinal Chemistry Letters, 30(18)

Authors

Blum, Eliav

Zhang, Jianye

Korshin, Edward

et al.

Publication Date

2020-09-15

DOI

10.1016/j.bmcl.2020.127421

Peer reviewed



HHS Public Access

Author manuscript

Bioorg Med Chem Lett. Author manuscript; available in PMC 2021 September 15.

Published in final edited form as:

Bioorg Med Chem Lett. 2020 September 15; 30(18): 127421. doi:10.1016/j.bmcl.2020.127421.

Development of chiral fluorinated alkyl derivatives of emixustat as drug candidates for the treatment of retinal degenerative diseases

Eliav Blum^a, Jianye Zhang^b, Edward Korshin^a, Krzysztof Palczewski^{b,c}, Arie Gruzman^{a,*}

^aDepartment of Chemistry, Faculty of Exact Sciences, Bar-Ilan University, Ramat-Gan 5290002, Israel

^bGavin Herbert Eye Institute, Department of Ophthalmology, University of California, Irvine, California, 92697, USA

^cDepartments of Physiology and Biophysics, and Chemistry, University of California, Irvine, California, 92697, USA

Abstract

The discovery of how a photon is converted into a chemical signal is one of the most important achievements in the field of vision. A key molecule in this process is the visual chromophore retinal. Several eye diseases are attributed to the abnormal metabolism of retinal in the retina and the retinal pigment epithelium. Also, the accumulation of two toxic retinal derivatives, N-retinylidene-N-retinylethanolamine and the retinal dimer, can damage the retina leading to blindness. RPE65 (Retinal pigment epithelium-specific 65 kDa protein) is one of the central enzymes that regulates the metabolism of retinal and the formation of its toxic metabolites. Its inhibition might decrease the rate of the retina's degeneration by limiting the amount of retinal and its toxic byproducts. Two RPE65 inhibitors, (R)-emixustat and (R)-MB001, were recently developed for this purpose.

Here we describe eleven steps-synthesis of the chiral fluorinated alkyl derivatives of emixustat. Two final compounds (enantiomers) showed significant inhibition of RPE-65 at a 2-fold lower concentration compared with (R)-MB001, one of the developed compounds caused 100% cell protection under all-trans-retinal treatment and both molecules showed equal potency as racemic emixustat. Such molecules might be used as drug candidates for developing novel treatments against retinal degeneration.

*Corresponding Author: Phone: 972-54-7489041. gruzmaa@biu.ac.il.

Publisher's Disclaimer: This is a PDF file of an unedited manuscript that has been accepted for publication. As a service to our customers we are providing this early version of the manuscript. The manuscript will undergo copyediting, typesetting, and review of the resulting proof before it is published in its final form. Please note that during the production process errors may be discovered which could affect the content, and all legal disclaimers that apply to the journal pertain.

ASSOCIATED CONTENT

Materials, synthetic procedures, NMR spectroscopic data, mass spectroscopy data, HPLC separation/purification-related information, and a description of the enzymatic assay are presented in the supplemental information file.

Declaration of interests

The authors declare that they have no known competing financial interests or personal relationships that could have appeared to influence the work reported in this paper.

One of the most fascinating biological processes in nature is the ability of living organisms to transform photonic signals into chemical and electrical ones. This is followed by analysis of the data and its interpretation in the brain¹. In mammals, the organ that is responsible for such information is the retina. Two types of photoreceptor cells are found in the retina; the rods and the cones, which are situated in a matrix of the retinal pigment epithelium (RPE). The RPE plays an important role in the chemistry of the visual cycle¹. The first step in the conversion of a photon into a chemical signal is its absorption in 11-cis-retinilidene, coupled with an opsin protein (rhodopsin and cone opsins), into all-trans-retinilidene^{2,3}. As a result, the opsin G protein-coupled receptor (GPCR) changes its conformation, leading to a signal transduction cascade and electrical events that end in the visual cortex of the brain. In order to sustain this process, a chain of chemical reactions needs to occur to restore 11-cis-retinilidene. This process includes the transformation of all-trans retinal to 11-cis retinol. The RPE65 enzyme plays a critical role in this process. Recycled 11-cis-retinal then travels back to the outer segments of the photoreceptors where, by conjugating with opsin, it forms rhodopsin in rod cells and generally three types of cone visual pigments^{2,3}. In some individuals, all-trans-retinal may be a precursor of two other toxic compounds: N-retinylidene-N-retinylethanolamine (A2E) and retinal dimer. An excess accumulation of these moieties may lead to the destruction of cells in the retina and to decreased visual ability^{4,2}. Such retinal degeneration is responsible for a large percentage of blindness and visual impairment. For example, age-related macular degeneration (AMD) is believed to account for 5% of global blindness⁵, and Stargardt disease appears in 1 out of 8,000–10,000 individuals in the US⁶.

Some novel drug design approaches for treatment of retinal degenerative diseases have focused on the development of RPE65 inhibitors. Such compounds might decrease the rate of the regeneration of all-trans-retinal in the retina and as result, reduce the production and the accumulation of A2E and/or retinal dimer. This, however, should be performed in a very precise manner, because over-suppression of the visual cycle might lead to augmentation of blindness and other degrees of sight impairment. For example, inhibition of 11-cis retinol formation in mice causes symptoms similar to Leber congenital amaurosis (LCA) and vitamin A deprivation⁷. Therefore, the optimal therapeutic use of RPE65 inhibitors to impede retinal degeneration should not aim for the complete prevention of visual chromophore regeneration, rather its partial inhibition⁸.

A known RPE65 inhibitor, (R)-emixustat, which is derived from retinylamine (Ret-NH₂)⁷ (see Figure 1), is currently undergoing clinical trials against retinal degeneration⁶. In addition to its activity as a RPE-65 inhibitor, the primary amine located in the molecule forms a Schiff base with the aldehyde group in all-trans-retinal, and by such a conjugation reduces its amount in the retina (see Figure 2)^{7,2,8}.

Here we describe the synthesis of the chiral fluorinated alkyl derivatives of emixustat. We present the complete synthesis of such compounds (Scheme 1). Thirteen new molecules (final and intermediates) were generated in the scope of this work. Both final compounds (two enantiomers) ((R/S)-3-amino-1-(3-((5-fluoro-2-(3-fluoropropyl) pentyl) oxy) phenyl) propan-1-ol, **14**, and (S/R)-3-amino-1-(3-((5-fluoro-2-(3-fluoropropyl) pentyl) oxy) phenyl) propan-1-ol, **15**) showed significant inhibition of RPE65 at lower concentrations

(approximately 2-fold), compared with the known RPE65 inhibitor (*R*)-MB001⁹ and showed equal potency as racemic emixustat.

Today, more than 50% of the blockbuster drugs are fluorinated compounds¹⁰. There are several significant reasons for this. First, fluorine is small, with a low atomic weight, and it has the highest electronegativity. These characteristics make the C-F bond highly polarized and strong, which can be used to hinder the metabolism of the drug in the body. Second, the three nonbonding electron pairs of fluorine, together with its high electronegativity, can be utilized to form more dynamic electrostatic interactions than can be attained with hydrogen atoms. Third, introducing a fluorine atom to a compound generally results in an increase in the lipophilicity. Introducing a fluorine atom plays an important role in medicinal chemistry by increasing the potential of metabolic oxidation, pKa, molecular recognition, lipophilicity, and conformation¹¹, while the modification has only minor effects on the shape and size of the molecule. These actions can improve the potency, absorption, selectivity, and the metabolism of a drug candidate¹¹.

It is also important to note that diastereo- and enantiomeric γ -aminoalcohol moieties are included in the structures of several drugs. These include, for example, 4-hydroxyleucine-based derivatives as anti-obesity drugs, ritonavir and lopinavir as anti-HIV drugs¹², and atomoxetine for attention deficit hyperactivity disorder (ADHD)¹³. It is therefore important to expand our knowledge of the synthetic methods, separation, purification, and the structural characterization of chirally resolved γ -aminoalcohols, which we will show in this work.

The first step towards the final products (compounds **14** and **15**, Scheme 1) was to synthesize 5-fluoro-2-(3-fluoropropyl)pentan-1-ol, compound **4** (Scheme 2). Dimethyl malonate was a starting material (Scheme 2, **step a**). The reaction was initiated with the dialkylation of dimethyl malonate by 1-fluoro-3-iodopropane, in the presence of NaH, in dry DMF, resulting in dimethyl 2,2-bis(3-fluoropropyl)malonate, compound **1** (100% yield)¹⁴. **Step b** in the reaction consisted of the hydrolysis of the two ester moieties of compound **1** by using trimethylsilanolate (NaOSi(Me)₃), in dry THF under reflux, resulting in the dicarboxylic acid derivative 2,2-bis(3-fluoropropyl)malonic acid, **2** (91% yield)¹⁵. Decarboxylation of **2** by Cu₂O in acetonitrile under reflux afforded monocarboxylic acid, 5-fluoro-2-(3-fluoropropyl)pentanoic acid, **3** in 98% yield¹⁶. Compound **3** was converted to alcohol **4** by reduction of the carboxylic acid moiety by LiAlH₄ (90% yield)¹⁷.

The preparation of 1-(3-((5-fluoro-2-(3-fluoropropyl)pentyl)oxy)phenyl)ethan-1-one, compound **6**, as an important intermediate for the entire synthesis, is shown in Scheme 3. First, the mesylation of the alcohol derivative **4** affords 5-fluoro-2-(3-fluoropropyl)pentyl methanesulfonate, compound **5**, in 100% yield.¹⁸ Second, fluorinated acetophenone **6** was obtained by creating the ether bond between commercially available 1-(3-hydroxyphenyl)ethan-1-one and compound **5** (91% yield).

The next synthetic step was performed using the Mannich reaction. A mixture of the fluorinated acetophenone **6**, (*S*)-(-)- α -methylbenzylamine, paraformaldehyde and HCl in 1,4-dioxane in a sealed tube were reacted, resulting in the Mannich base, (*S*)-1-(3-((5-

fluoro-2-(3-fluoropropyl)pentyl)oxy)phenyl)-3-((1-phenylethyl)amino)propan-1-one, **7**, in 38% yield (see Scheme 4) based on¹⁹. The insertion of an (S)-chiral center into compound **7** using (S)-(-)- α -methylbenzylamine allows the formation of the two diastereomers in the next step. Using this method, it was possible to avoid the chiral separation of the diastereomers and to obtain the final desired compounds in a simpler and cheaper way.

Scheme 5 shows how the Mannich base **7** was reduced with NaBH₄ in MeOH to obtain two γ -amino alcohol diastereomers, 1-(3-((5-fluoro-2-(3-fluoropropyl)pentyl)oxy)phenyl)-3-(((S)-1-phenylethyl)amino)propan-1-ol, **8**.

Several attempts to separate these diastereomers by normal phase flash chromatography (FC) were unsuccessful. This is probably due to the high affinity of the amine and the hydroxyl groups to the silica phase. Hence, the diastereomers **8** (see Scheme 6) were reacted with 1,1'-carbonyldiimidazole (CDI) in THF to form the carbamate cyclization diastereomers, 6-(3-((5-fluoro-2-(3-fluoropropyl)pentyl)oxy)phenyl)-3-((S)-1-phenylethyl)-1,3-oxazinan-2-one, **9** (85% yield)²⁰. This cyclization facilitated the separation by normal-phase FC. Compounds (R/S)-6-(3-((5-fluoro-2-(3-fluoropropyl)pentyl)oxy)phenyl)-3-((S)-1-phenylethyl)-1,3-oxazinan-2-one, **10**, and (S/R)-6-(3-((5-fluoro-2-(3-fluoropropyl)pentyl)oxy)phenyl)-3-((S)-1-phenylethyl)-1,3-oxazinan-2-one, **11**, were separated easily, resulting in 36% and 45% yields, respectively. The separated diastereomers **10** and **11** were reacted with KOH to open the carbamate cyclization and to form the fluorinated γ -amino alcohol diastereomers, (R/S)-1-(3-((5-fluoro-2-(3-fluoropropyl)pentyl)oxy)phenyl)-3-(((S)-1-phenylethyl)amino)propan-1-ol, **12**, (89% yield) and (S/R)-1-(3-((5-fluoro-2-(3-fluoropropyl)pentyl)oxy)phenyl)-3-(((S)-1-phenylethyl)amino)propan-1-ol, **13** (92% yield), respectively²¹. In the final step, compounds **12** and **13** were debenzylated with NH₄HCO₂ using 10% Pd/C in MeOH as a catalyst, resulting in two separated fluorinated γ -amino alcohols: **14** and **15** in 91% and 93% yield, respectively²².

Some of the above-mentioned procedures were planned after many failures and optimization attempts, which are listed below. The reader who is interested in conducting a similar synthesis might find this information useful.

- a. The dialkylation step used to form compound **1** (Scheme 2, **step a**): Initially, the starting material was diethyl malonate instead of dimethyl malonate. The use of t-BuOK as a base in the presence of 1-bromo-3-fluoropropane in t-BuOH under reflux overnight resulted only in monoalkylation. The use of NaH as a base instead, in the presence of 1-bromo-3-fluoropropane (2 or 3 eq), tert-butylammonium iodide (TBAI) in dry DMF at 100 °C overnight resulted in monoalkylation as well.

The monoalkylated product was reacted again under the latter conditions, resulting in the dialkylation of diethyl malonate. This reaction, occurring in two steps, consumed large amounts of the fluorinated compound, and was therefore abandoned. Eventually, diethylmalonate was replaced with dimethylmalonate, the reasons for which will be described in the next section (b). In parallel, the conditions mentioned in Scheme 1 **step a** were revised: the dimethyl malonate was reacted with 1-iodo-3-fluoropropane (2.5 eq)

because it is a better leaving group instead of 1-bromo-3-fluoropropane in dry DMF at only 60 °C overnight. Following these optimization steps, the dialkylated product **1** could be obtained in only one step and in 100% yield¹⁴.

- b.** The hydrolysis reaction in Scheme 1, step b began with preliminary attempts to perform both the hydrolysis and decarboxylation of diethyl 2,2-bis(3-fluoropropyl)malonate simultaneously using the following reagents: (1) Boric acid under reflux, resulting in no product²³; (2) LiOH in 2-methoxyethanol at 120 °C based on²⁴, resulting in a mixture of the monohydrolyzed product and the decarboxylation product; (3) LiCl in a DMSO/H₂O mixture under reflux (or in DMF at 120 °C) based on²⁵, resulting in many impurities and large amounts of the starting material; (4) 6N HCl at reflux²⁶, resulting in a mixture of the monohydrolyzed product and the decarboxylation product.

Such failures motivated us to separate the hydrolysis of the two ester groups as well as the decarboxylation. Following Lovrić et al.¹⁵, the hydrolysis step was performed by using NaOSi(Me)₃. This hydrolysis presumably occurs via an S_N2-type reaction by a nucleophilic attack of the anion of NaOSi(Me)₃ on the alkyl group carbon; therefore, diethyl 2,2-bis(3-fluoropropyl)malonate was replaced with dimethyl 2,2-bis(3-fluoropropyl)malonate **1**, as described in Scheme 2 **step a**. Compound **1** was thus reacted with NaOSi(Me)₃ in dry THF under reflux, and dicarboxylic acid **2** was easily obtained in high yield (91%), as previously reported¹⁵. The decarboxylation step was performed as a separate step, as described in Scheme 1, **step c** also resulting in a very good yield (98%)¹⁶.

Next, the ability of the final compounds **14** and **15** to inhibit the activity of RPE65 was examined (see Table 1). Two synthesized compounds, racemic emuxastate and (*R*)-MB001 were preincubated for 5 min at room temperature with bovine RPE microsomes⁸. All-*trans*-retinol was added, and the mixture was incubated at 37°C. Then, all the incubation mixtures were quenched by adding methanol after 1 hour of incubation, and the products were extracted with hexane. The production of 11-*cis*-retinol was quantified by normal-phase HPLC⁸. The concentrations of all four compounds were detected by monitoring its absorbance at 325 nm and quantified based on a standard curve representing the relationship between the amount of 11-*cis*-retinol and the area under the corresponding chromatographic peak. By this method, an inhibition of RPE65 enzymatic activity was measured as a function of the rate of the decrease of the 11-*cis*-retinol production.

Finally, the possible cytoprotective effect of the active compounds was tested in ARPE-19 cells, a spontaneously immortalized cell line of human retinal pigment epithelium²⁷. In Figure 3 is shown that the all active in the enzymatic assay compounds: emixustat, MB-001, compounds **14** and **15** caused significant positive effect on the cell viability in the presence of all-*trans*-retinal. However, it is important to mention that among all four tested compounds, only compound **14** was successful to keep the 100% of cell surveillance rate.

In conclusion, based on the emixustat scaffold, two fluorinated γ -amino alcohol derivatives ((*R/S*)-3-amino-1-(3-((5-fluoro-2-(3-fluoropropyl) pentyl) oxy) phenyl) propan-1-ol, **14** and (*S/R*)-3-amino-1-(3-((5-fluoro-2-(3-fluoropropyl) pentyl) oxy) phenyl) propan-1-ol, **15**) were synthesized in eleven synthetic steps. Both enantiomers effectively inhibited the

targeted enzyme, RPE65, in the nanomolar concentration range. Both compounds demonstrated a potency similar to that of the parent compound. However, they were two fold more potent when compared with (*R*)-MB001. In addition, both compounds showed significant cytoprotective effect in the presence of toxic concentrations of all-trans-retinal in ARPE65 cell.

Supplementary Material

Refer to Web version on PubMed Central for supplementary material.

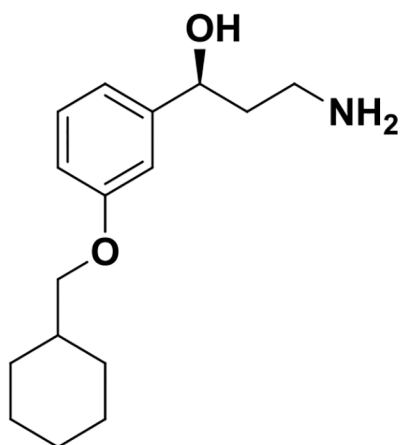
ACKNOWLEDGMENTS

This study was supported by a Bar-Ilan University new faculty grant (to A.G). This research was in part supported in part by grant to K.P. from the National Institutes of Health (NIH) EY009339. The authors also acknowledge support from an RPB unrestricted grant to the Department of Ophthalmology, University of California, Irvine, USA. Israel Ministry of Immigration and Integration through Kamea fellowship supported EEK (8279). We thank Dr. Huajun Yan for his help with the cell viability assay, and Mr. Steven Manch for the English editing. K. Palczewski is the Leopold Chair of Ophthalmology at the Gavin Herbert Eye Institute, Department of Ophthalmology, University of California, Irvine, USA.

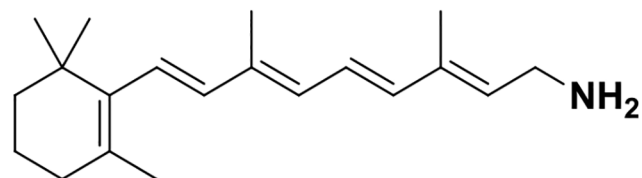
REFERENCES AND NOTES

1. Vera-Díaz FA; Doble N In Topics in Adaptive Optics; InTech, 2012; pp. 119–150.
2. Palczewski K Investigative ophthalmology & visual science 2014, 55, 6651–6672. [PubMed: 25338686]
3. Kiser PD; Golczak M; Palczewski K Chemical reviews 2014, 114, 194–232. [PubMed: 23905688]
4. Sparrow JR; Boulton M Experimental eye research 2005, 80, 595–606. [PubMed: 15862166]
5. Pascolini D; Mariotti SP British Journal of Ophthalmology 2012, 96, 614–618. [PubMed: 22133988]
6. Kubota R; Gregory J; Henry S; Mata NL Drug Discovery Today 2019, 25, 293–304.
7. Zhang J; Kiser PD; Badiie M; Palczewska G; Dong Z; Golczak M; Tochtrop GP; Palczewski K The Journal of clinical investigation 2015, 125, 2781–2794. [PubMed: 26075817]
8. Zhang J; Dong Z; Mundla SR; Hu XE; Seibel W; Papoian R; Palczewski K; Golczak M Molecular pharmacology 2015, 87, 477–491. [PubMed: 25538117]
9. Kiser PD; Zhang J; Badiie M; Li Q; Shi W; Sui X; Golczak M; Tochtrop GP; Palczewski K Nature chemical biology 2015, 11, 409–415. [PubMed: 25894083]
10. Mei H; Han J; Fustero S; Medio-Simon M; Sedgwick DM; Santi C; Ruzziconi R; Soloshonok VA Chemistry–A European Journal 2019, 25, 11797–11819.
11. Swallow S In Progress in medicinal chemistry; Elsevier, 2015; pp. 65–133.
12. Verkade JM; Quaedflieg PJ; Verzijl GK; Lefort L; van Delft FL; de Vries JG; Rutjes FP Chemical Communications 2015, 51, 14462–14464. [PubMed: 26273707]
13. Sauer J-M; Ring BJ; Witcher JW Clinical pharmacokinetics 2005, 44, 571–590. [PubMed: 15910008]
14. Hoshino T; Watanabe J. i.; Kudo M; Sakai E; Funyu S; Ishitsuka K. i.; Okamoto S Journal of Polymer Science Part A: Polymer Chemistry 2012, 50, 1707–1716.
15. Lovri M; Capanec I; Litvi M; Bartolin i A; Vinkovi V Croatica chemica acta 2007, 80, 109–115.
16. Toussaint O; Capdevielle P; Maumy M Synthesis (Stuttgart) 1986, 1029–1031.
17. Chow H-F; Ng K-F; Wang Z-Y; Wong C-H; Luk T; Lo C-M; Yang Y-Y Organic letters 2006, 8, 471–474. [PubMed: 16435862]
18. Gallardo H; Conte G; Bryk F; Lourenço MCS; Costa MS; Ferreira VF Journal of the Brazilian Chemical Society 2007, 18, 1285–1291.

19. Wang J; Wang Y; Liu D; Zhang W *Advanced Synthesis & Catalysis* 2015, 357, 3262–3272.
20. Ella-Menye J-R; Sharma V; Wang G *The Journal of organic chemistry* 2005, 70, 463–469. [PubMed: 15651787]
21. Davies SG; Haggitt JR; Ichihara O; Kelly RJ; Leech MA; Mortimer AJP; Roberts PM; Smith AD *Organic & biomolecular chemistry* 2004, 2, 2630–2649. [PubMed: 15351828]
22. Ram S; Spicer LD *Synthetic Communications* 1987, 17, 415–418.
23. Wehrli PA; Chu V *The Journal of Organic Chemistry* 1973, 38, 3436–3436.
24. Ogawa K; Sasaki M; Nozaki T *Applied radiation and isotopes* 1997, 48, 623–630.
25. Williams RM; Glinka T; Kwast E; Coffman H; Stille JK *Journal of the American Chemical Society* 1990, 112, 808–821.
26. Grote J; Chen Y-Y *Tetrahedron Letters* 2014, 55, 676–678.
27. Dunn K; Aotaki-Keen A; Putkey F; Hjelmeland LM *Experimental eye research* 1996, 62, 155–170. [PubMed: 8698076]



(R)-emixustat



Ret-NH₂

Figure 1.
RPE65 inhibitors⁷.

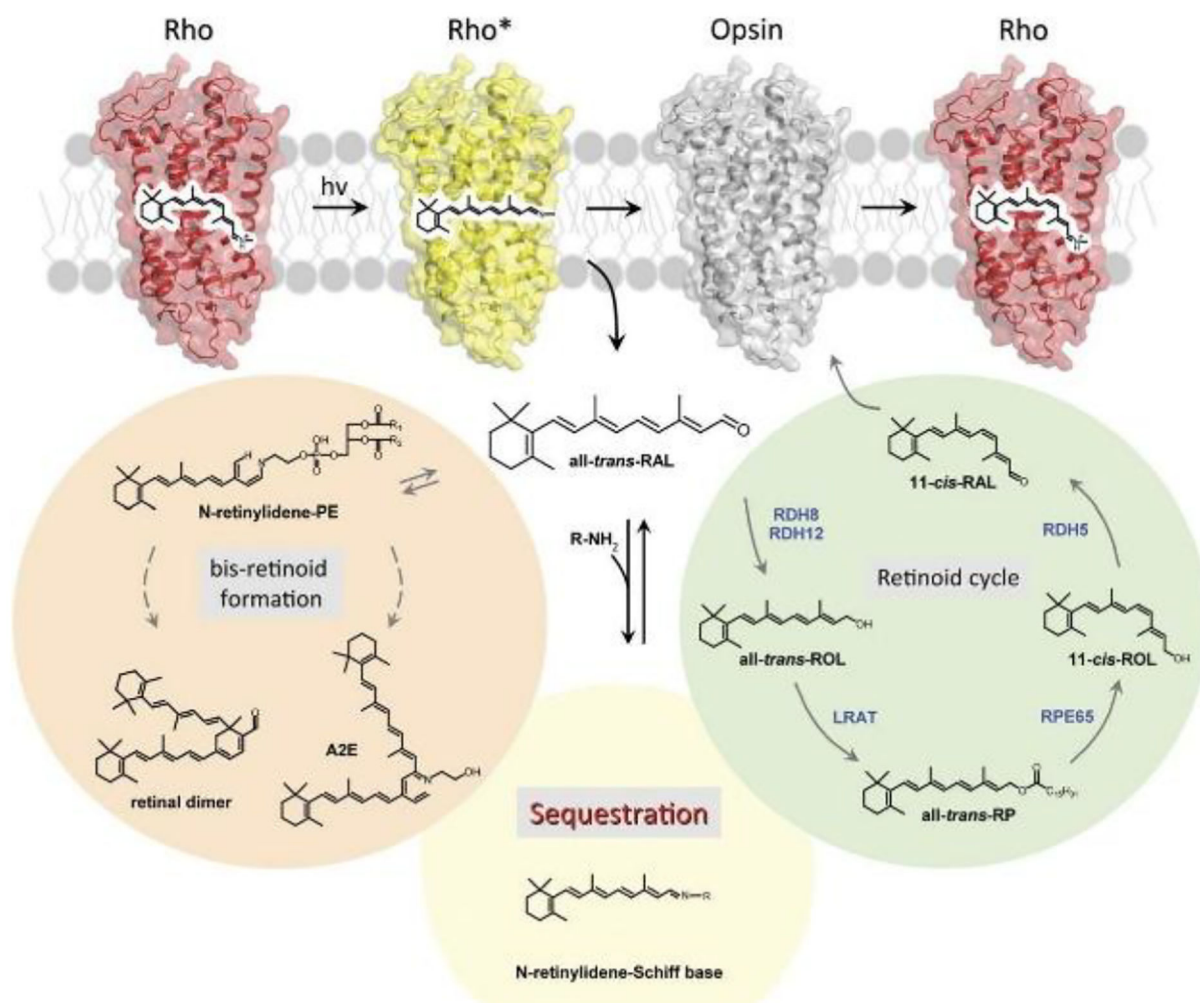


Figure 2. All-trans-retinal sequestration; preventing the accumulation of retinal condensation products².

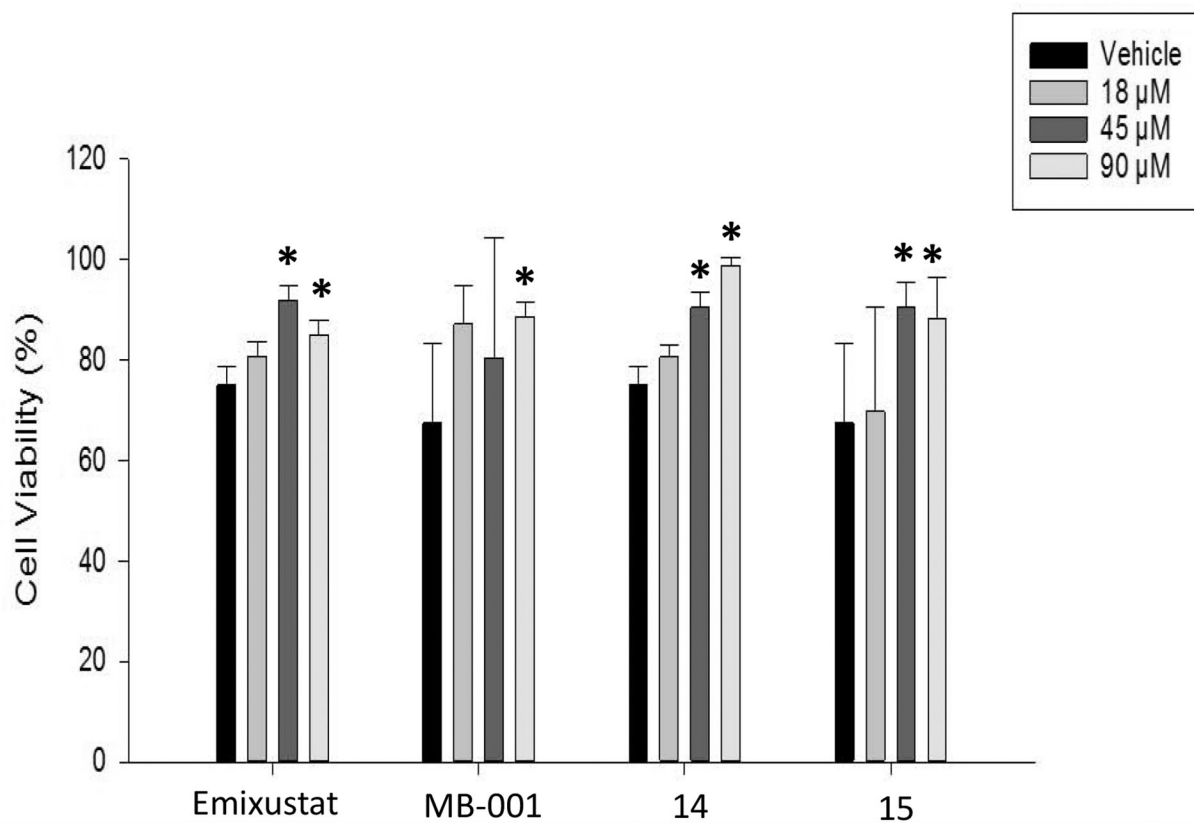
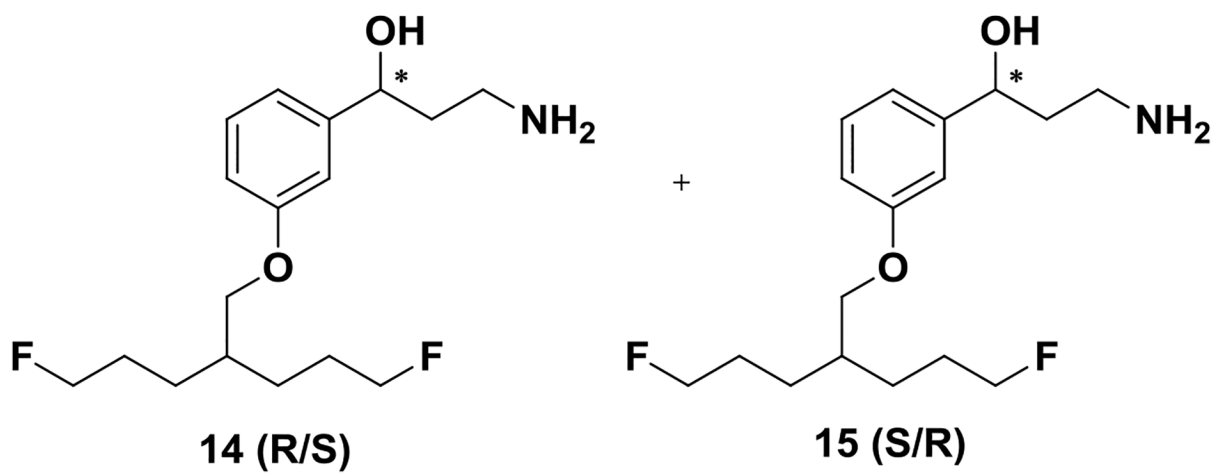
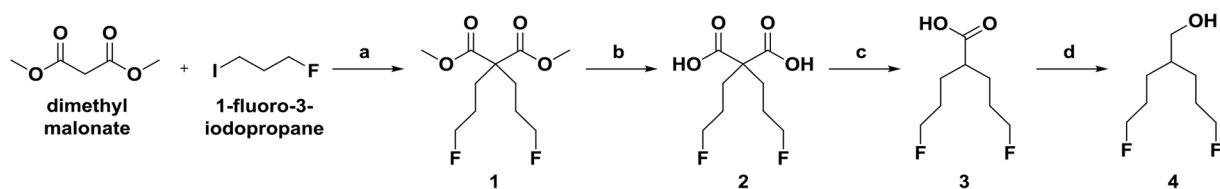


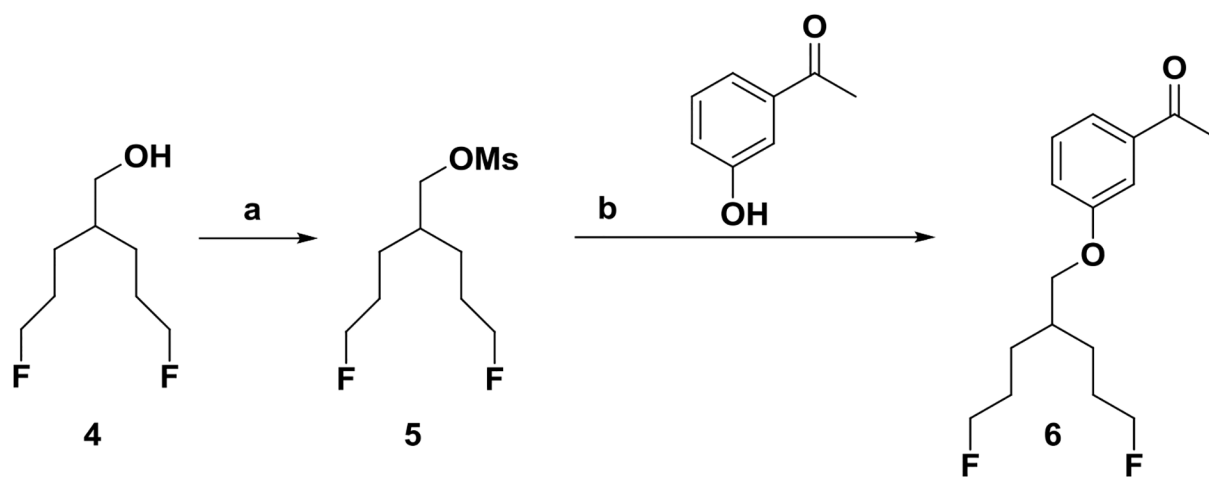
Figure 3.

Protection of ARPE65 cell by RPE65 inhibitors. ARPE-19 cells were treated with 18, 45 and 90 μM of emixustat, MB-001, compounds; **14** and **15**. All-trans-retinal in concentration of 385 μM was added to the relevant groups, together with the addition of the test compounds. Cell viability was measured over 6 h incubation at 37 °C. CellTiter-Glo luminescent cell viability assay was used, according to the manufacturer protocol. MEAN ±SE, n=3, t-test was used for the statistical evaluation.



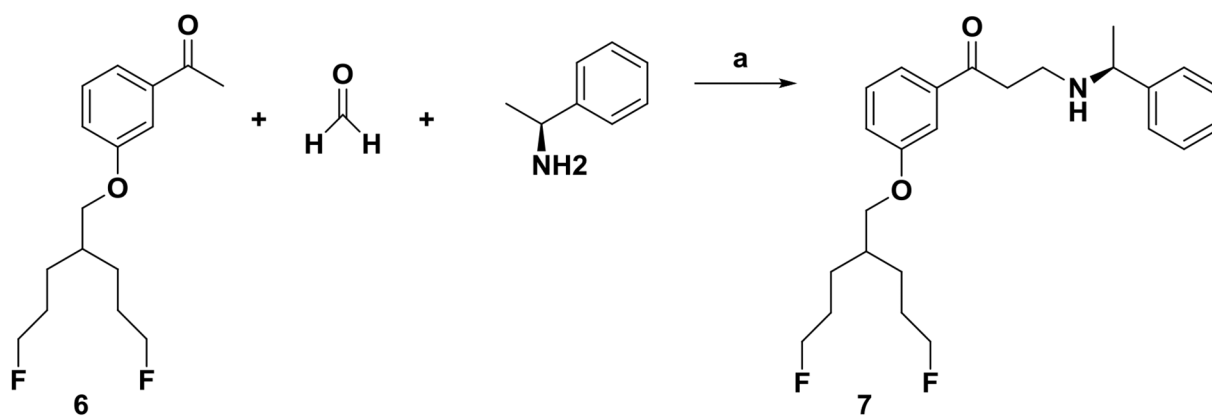
Scheme 1:
The final desired inhibitors

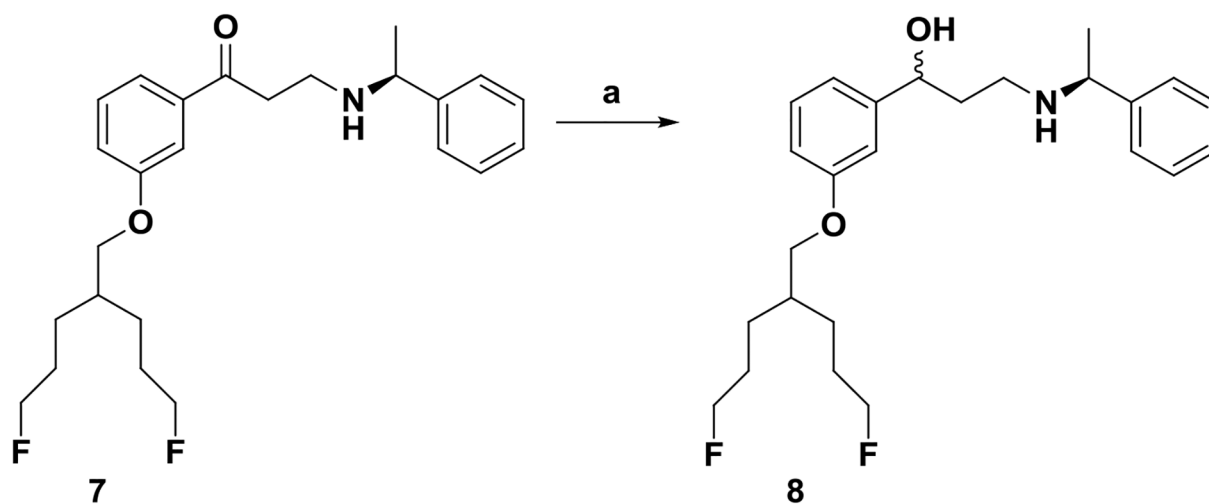
**Scheme 2.**Synthesis of the fluorinated alcohol chain^a^aReagents and conditions: (a) NaH, dry DMF, 0 °C to 60 °C, overnight; (b) NaOSi(Me)₃, dry THF, reflux, overnight; (c) Cu₂O, acetonitrile, reflux, 18 h; (d) LiAlH₄, dry THF, 0 °C, 4 h.

**Scheme 3.**

Synthesis of fluorinated alkoxy acetophenone by the mesylation of an alcohol chain^a

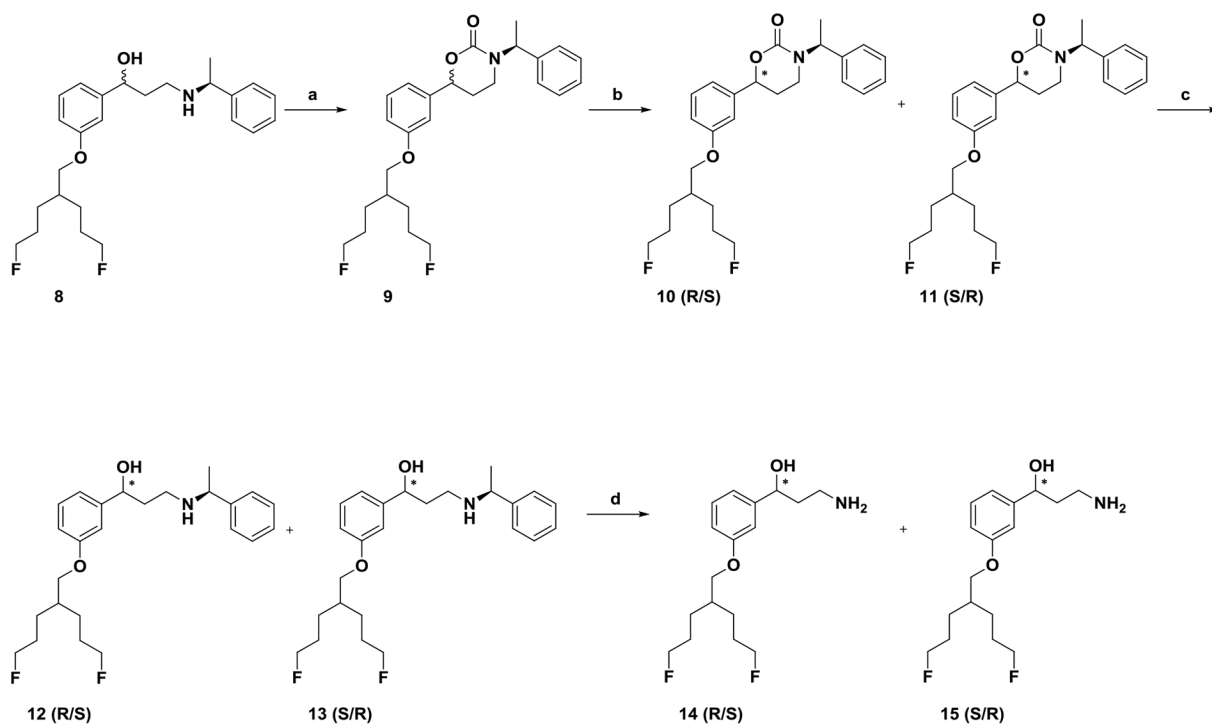
^aReagents and conditions: (a) MsCl, TEA and DCM, at 0 °C to room temperature, 2h and 15 min; (b) K₂CO₃, DMF, 0 °C to 85 °C, 2h and 15 min.

**Scheme 4.**Mannich reaction of the fluorinated alkoxy acetophenone^a^aReagents and conditions: (a) paraformaldehyde, HCl and 1,4-dioxane, pressure tube, at 110 °C, for 16h.

**Scheme 5.**

The diastereomers obtained after Mannich base reduction^a

^aReagents and conditions: (a) NaBH₄ and MeOH, at room temperature, for 1.5 h.

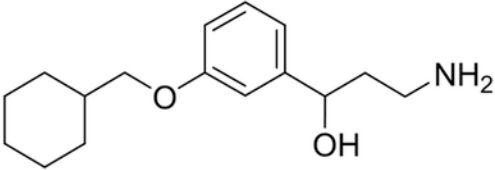
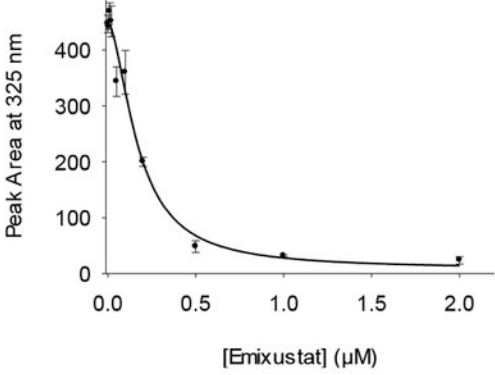
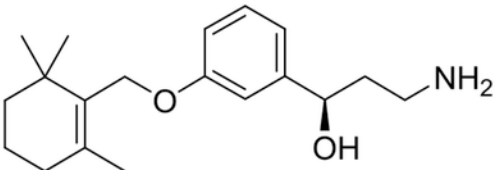
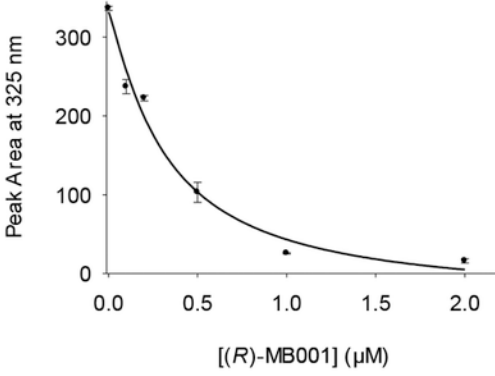
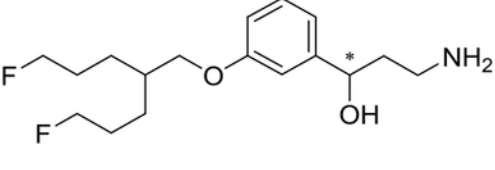
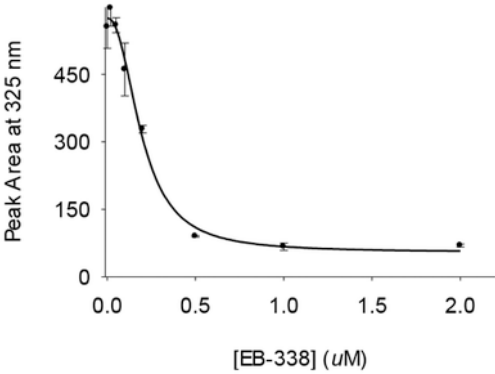
**Scheme 6.**

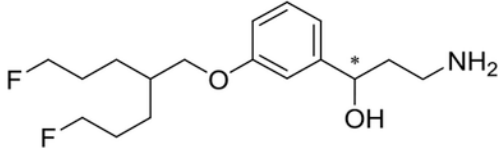
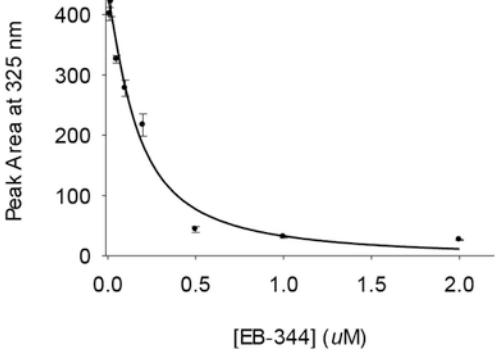
The diastereomers' separation and debenzoylation to obtain the desired products^a

^aReagents and conditions: (a) CDI and THF, reflux, for 12 h; (b) FC purification; (c) KOH and H₂O:EtOH (1:1), reflux, overnight; and (d) NH₄HCO₂, 10% Pd/C and MeOH, reflux, for 2 h.

Table 1.

Inhibition of the RPE65 activity

Name	Structure	Inhibition	EC50 (nM)
Racemic-emixustat			172.4 ± 29.3
(<i>R</i>)-MB001			323.3 ± 14.59
14			196.5 ± 17.9

Name	Structure	Inhibition	EC50 (nM)																
15		 <table border="1"><caption>Approximate data points from the inhibition curve</caption><thead><tr><th>[EB-344] (µM)</th><th>Peak Area at 325 nm</th></tr></thead><tbody><tr><td>0.0</td><td>400</td></tr><tr><td>0.1</td><td>320</td></tr><tr><td>0.2</td><td>280</td></tr><tr><td>0.3</td><td>220</td></tr><tr><td>0.5</td><td>100</td></tr><tr><td>1.0</td><td>50</td></tr><tr><td>2.0</td><td>30</td></tr></tbody></table>	[EB-344] (µM)	Peak Area at 325 nm	0.0	400	0.1	320	0.2	280	0.3	220	0.5	100	1.0	50	2.0	30	
[EB-344] (µM)	Peak Area at 325 nm																		
0.0	400																		
0.1	320																		
0.2	280																		
0.3	220																		
0.5	100																		
1.0	50																		
2.0	30																		

Author Manuscript

Author Manuscript

Author Manuscript

Author Manuscript